

PAPER • OPEN ACCESS

## Finite element modelling of independent core propagation in multicore photonic crystal fibres resulting from anisotropy in structure

To cite this article: M Mohammed and A K Ahmad 2021 *J. Phys.: Conf. Ser.* **1736** 012037

View the [article online](#) for updates and enhancements.

### You may also like

- [New generation of optical fibres](#)  
E.M. Dianov, S.L. Semjonov and I.A. Bufetov
- [A method for measuring coupling coefficients between cores and corrections to mode propagation constants in multicore fibres](#)  
N.A. Kalinin, A.V. Andrianov and A.V. Kim
- [Multicore optical fibre embedded Fabry–Perot sensing element of a bend sensor](#)  
O.N. Egorova, S.G. Zhuravlev, V.I. Pustovoy et al.



**ECS**  
The  
Electrochemical  
Society  
Advancing solid state &  
electrochemical science & technology

**DISCOVER**  
how sustainability  
intersects with  
electrochemistry & solid  
state science research

# Finite element modelling of independent core propagation in multicore photonic crystal fibres resulting from anisotropy in structure

M Mohammed<sup>1,2</sup> and A K Ahmad<sup>3</sup>

<sup>1</sup> Department of Physics, Institute of Applied Physics, University of Muenster, Corrensstr. 2-4, 48149 Muenster, Germany.

<sup>2</sup> Department of Physics, University of Al-Mustansiriyah, College of Science, Baghdad, Iraq.

<sup>3</sup> Department of Physics, Al-Nahrain University, College of Science, Baghdad, Iraq.

m\_moha05@uni-muenster.de ahmad.kamal@sc.nahrainuniv.edu.iq

**Abstract.** COMSOL MULTIPHYSICS software based on the finite element method is being used to simulate the random anisotropy in diameters of the cores formed in multicore photonic crystal fibre structures, and this may affect the coupling properties between the cores' modes. Consequently, this leads to a reduction in the coupling efficiency between the cores with different structures. This anisotropy in diameters of the cores leads to the creation of a small mismatch between the modes of these cores and is sufficient to inhibit coupling. The coupling properties are affected hugely depending on the amount of the change in core diameter and increasing the number of cores coupled inside the multicore structure. We also found an improvement in the coupling efficiency when increasing the number of cores within the structure of the multicore photonic crystal fibres; otherwise, the independent light propagation of each core inside the multicore structure, with/without a little penetration with other adjacent cores. As the coupling efficiency of seven-core coupled is better than three-core, and the latter may be better than two-core in which the cores appear decoupled and independent in their propagated for the adjacent other cores. It can be considered this study a novel characteristic of multiplexing-demultiplexing applications.

## 1. Introduction

These Photonic crystal fibres (PCFs) possess flexible design and unique propagation properties that are not realized in conventional optical fibre, offering many possibilities for fibre-based devices [1, 2]. They consist of an array of air holes running along the fibre length and guiding light by total internal reflection (TIR) between the solid core and the cladding region with multiple air-holes [2, 3]. The usual PCF consists of one defect in the central region and the light guided along with this defect [2, 4]. Recently, PCF with two adjacent defect regions (served as two core), called multicore PCFs (MCPCF) [2, 5]. It is a possibility to use it as an optical fibre coupler [6-12]. These PCF couplers with identical two cores possess the possibility of achieving a multiplexer- demultiplexer [2, 5]. Destroying the symmetry of the PCF couplers is the key method to obtain anisotropy in the structure. In general, one can introduce asymmetry in the structure by using different dimensions of the coupler or variation between the cores or using different index profiles [13, 14]. Here, to demonstrate our method, we assume that the index profiles for all cores of the coupler are the same,



Content from this work may be used under the terms of the [Creative Commons Attribution 3.0 licence](https://creativecommons.org/licenses/by/3.0/). Any further distribution of this work must maintain attribution to the author(s) and the title of the work, journal citation and DOI.

and we introduce a change in all core diameters of the coupler to become all non-identical, leads to unequal power distribution in each core. The non-identical coupler can be also used for applications such as coupler [1, 10, 12, 14, 15], polarization beam splitter [16], switcher [17], multiplexer-demultiplexer MUX-DEMUX [13, 18-20].

In our study, we design different geometrical structures, such as two-, three-, and seven-core PCFs coupler to predict the mode behaviour in several of coupled MCPCF. Which have the potential to affect the coupling properties between coupled cores, such that reduction of the coupling significantly, so that the coupling non-existent between the cores and then the cores become decoupled, consequently propagates the light independently essentially in all cores, as individual cores. In isolation, we present our theoretical study using COMSOL MULTIPHYSICS software based on a finite element method (FEM) to prove the accuracy numerical of this method to simulate an MCPCF.

## 2. Theory

We begin our analysis by designing different structures such as two-, three-, and seven-core as the MCPCF system. First, assume that we have an N-core MCPCF. We assume that the propagation constant of each core is  $\beta_0$ ; the coupling coefficient between the cores is  $\kappa_{0n}$ , the evolution of the modal field amplitudes in MCPCF coupler as  $U_0$  can be described 'as in equation (1)' [13, 21, 22]:

$$i \frac{dU_0}{dz} + \beta_0 U_0 + \kappa_{0n} \sum_{n=1}^N U_n = 0 \quad (1)$$

Eigenvalues associated with the amplitude of the field at the nth core is  $U_n = u_n \exp(i\beta_0 z)$ . The coupling coefficients among different cores can calculate 'as in equation (2)' [13, 19, 20]:

$$\kappa_{0n} = (2\Delta_n)^{1/2} \frac{U_0 U_n}{R_0 V_0} \times \frac{K_0(W_0 D_{0n} / R_0)}{K_1(W_0) K_1(W_n)} \times \frac{\bar{W}_0 K_0(W_n) I_1(\bar{W}_0) + W_n K_1(W_n) I_0(\bar{W}_0)}{\bar{W}_0^2 + U_n^2} \quad (2)$$

Where  $\kappa_{0n}$  between the core 0 and n, the waveguide index difference is  $\Delta_n = (n_{1,n} - n_{2,n}) / n_{1,n}$ , and  $n_{1,n}$ , and  $n_{1,2}$  are the refractive indices of the core and cladding, respectively.  $V_0 = k_0 R_0 n_{1,0} (2\Delta_0)^{1/2}$  is the dimensionless frequency number for the central core 0,  $W_0 = R_0 (\beta_0^2 - k^2 n_{2,0}^2)^{1/2}$ ,  $U_0 = R_0 (k^2 n_{1,0}^2 - \beta_0^2)^{1/2}$ , The propagation constant  $\beta$  can be defined from the eigenvalue problem by  $V^2 = W^2 + U^2$ . While  $\bar{W}_0 = W_0 R_n / R_0$ ,  $I_{n(x)}$  and  $k_{n(x)}$  both are the modified Bessel functions of the first and second kind, respectively.  $k$  refers to is the free-space wavenumber, and both of  $D_{0,n}$ , and  $R_0$  refer to the distance between core centres for 0 and n, and the core radii. The power flow as a function of z is defined from by the Poynting vector using 'as in equation (3) [1]:

$$P_{core}(z) = 1/2 \text{Re} \iint_{corearea} \vec{E}(x, y, z) \vec{H}(x, y, z) \cdot \hat{z} dx dy \quad (3)$$

Where the guided fields are determined from the equation (1)

FEM solver can analyse the guided modes of two, three, and seven-core PCF by directly solving Maxwell's equation [4, 6, 7, 9, 19-20]. Then, we get an approximate value of the effective refractive mode index [7, 19], as mentioned in equation (4) that represents the vectorial wave equation for the electric field E using COMSOL software based on FEM for

modelling the mode analysis and determine the effective refractive indices of modes for all structure ‘as in equation (4)’ shown below:

$$\nabla \times (\nabla \mu_r^{-1} \times E) - k_0^2 \epsilon_r E = 0 \quad (4)$$

Here  $k_0$  is the free space wavenumber, permeability and permeability of the material represent by  $\mu_r$  and  $\epsilon_r$  with  $\epsilon_r = n - ik$  and  $n$  represents the real part of the refractive index,  $\lambda = j\beta - \sigma z$ . By assuming that the multicore PCF is non-magnetic and non-conducting, i.e.,  $\mu_r = 1$  and  $\sigma = 0$ . The FEM method is utilized to solve light propagation in MPCFs due to its ability to simulate complex engineering structures and because it allows us to divide the cross-section of PCF into a finite triangle mesh that can be different in sizes and shapes [7, 19]. The refractive mode indexes and modal field distributions are evaluated. Then, the distributions of the power flow as a function of  $z$  in each core of two, three, and seven- cores of MCPC are determined.

### 3. Design mythology

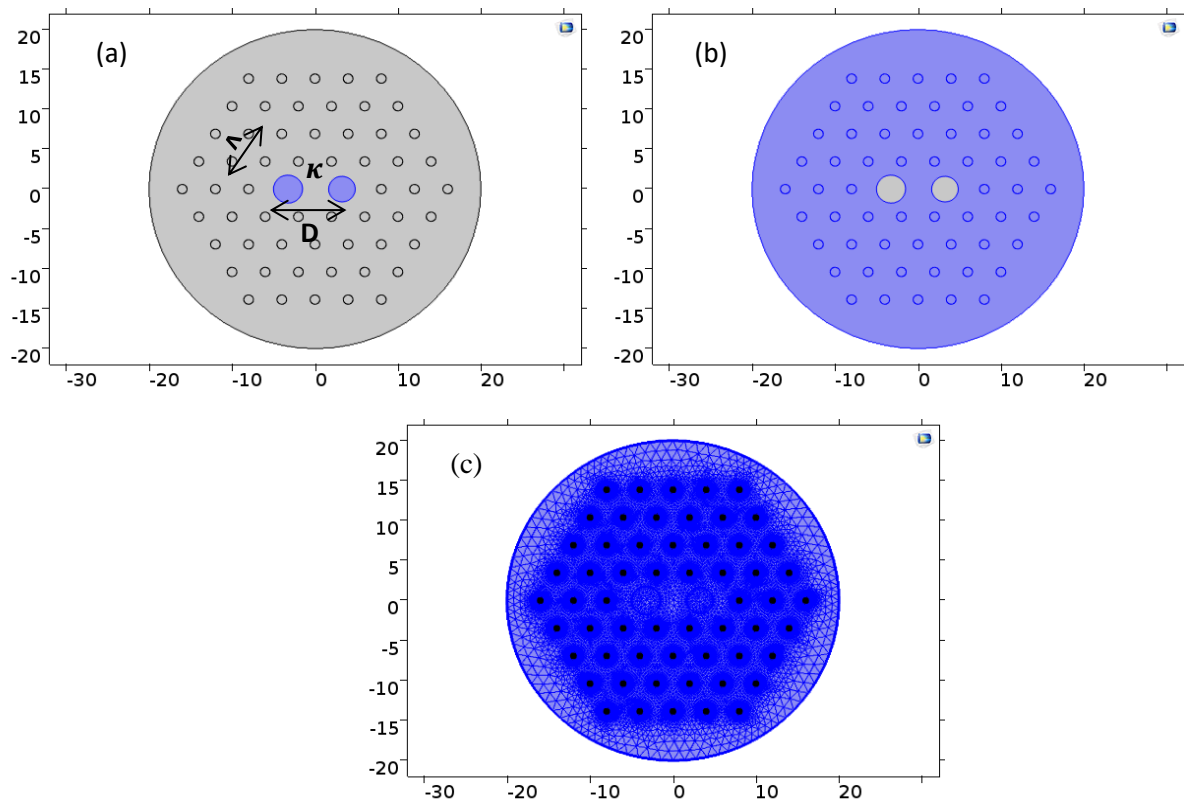
We are designing the methodology using COMSOL MULTIPHYSICS software that based FEM to engineer structures with different configurations, such as two, three, and seven-core with introducing a random anisotropy in all core diameters for these structures. The diameters of the cores were in the different structures as follows, for a structure consisting of two cores with diameters such as 3.2  $\mu\text{m}$  and 3.5  $\mu\text{m}$ , while a structure consisting of three cores with diameters would be like 3.2  $\mu\text{m}$ , 3.5  $\mu\text{m}$ , 3.8  $\mu\text{m}$ . As for the structure consisting of seven cores with diameters such as 3.2  $\mu\text{m}$ , 3.47  $\mu\text{m}$ , 3.48  $\mu\text{m}$ , 3.49  $\mu\text{m}$ , 3.5  $\mu\text{m}$ , 3.51  $\mu\text{m}$ , and 3.52  $\mu\text{m}$ , respectively. The refractive index of silica core is 1.45 is slightly higher than the refractive index of cladding 1.4 at a wavelength of 1.55  $\mu\text{m}$ , with the structural parameters are the hole diameter  $d = 1.16 \mu\text{m}$ ; the pitch is  $\Lambda = 4 \mu\text{m}$ , core separation  $D = 2.5\Lambda$  at a wavelength of 1.55  $\mu\text{m}$ , as in figure 1, figure 2, figure 3, that show represents the engineering design of three different structures in terms of the formation, such as two, three, and seven-core, then, we material insertion of the core and cladding as in figure 1 (a) and (b), figure 2 (a) and (b), figure 3 (a) and (b) of the figure. Then we choose the physical model as the electromagnetic waves-domain frequency to study the mode analysis, then, we set the boundary condition like a perfectly matched layer (PML). FEM allows us to divide the cross-section of two, three, seven-core PCF structures into small finite elements by using mesh-free triangular (maximum and minimum element size of mesh are 2.68  $\mu\text{m}$  and 0.012 with curvature factor 0.3) as in figure 1, figure 2, figure 3 (c) of the two-, three-, and seven cores. After that, we select the study as the mode analysis.

### 4. Simulation results and discussion

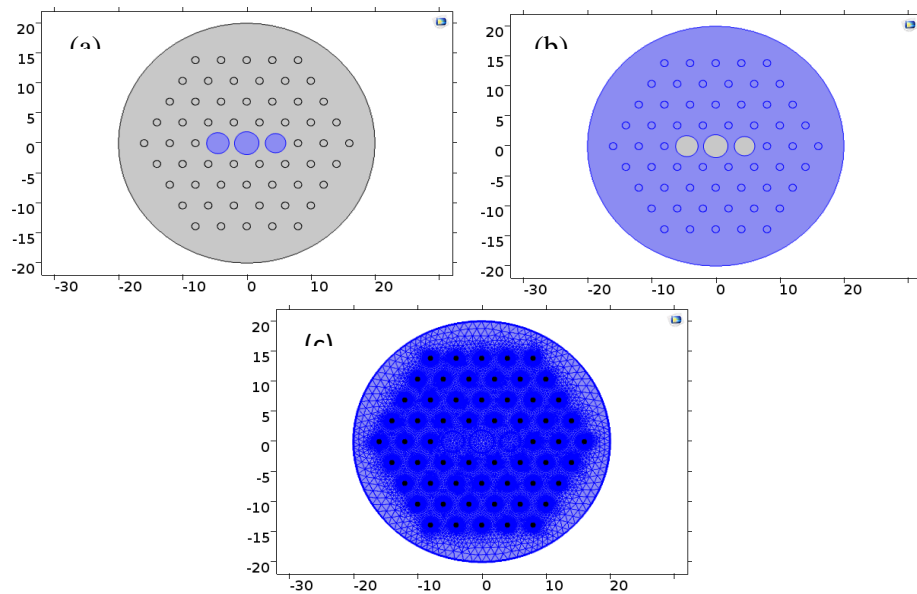
Using COMSOL Multiphysics software that based on FEM, we modelled carry out simulated by introducing a small and random anisotropy in cores diameters whatever their structure, i.e., we change the diameters of all cores a little bit more than others, to see intuitively how this affects the coupling properties between the cores of MCPCF with different structures. The numerical results from the simulation presented as in figure 4, figure 6, and figure showed how affected the coupling properties between cores in different structures. As a result, in occurring a slight change in cores diameters of MCPCF become each core diameter differing adjacent cores diameters for it and this leads to a small mismatch between the modes of these cores. In turn, prevents the coupling between these cores, the cores become decoupled, and independent in the light propagation from their neighbours.

Although, the anisotropy in all core diameters essentially reduces the coupling efficiency between cores, where the modes of these cores become decoupled from their adjacent, and hence these cores remain in isolation in their structure. On the other hand, we noticed from the

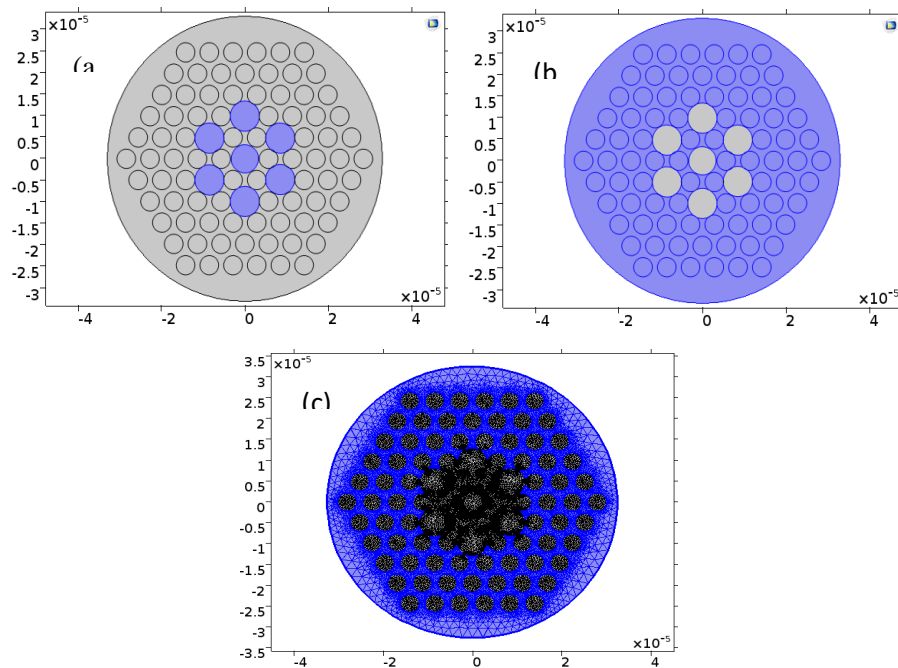
results; there is an improvement in the coupling efficiency when increased the number of cores within the MCPCF structure, as figure 4, figure 6, figure 8, and their equivalent as figure 5, figure 7 and figure 9. From these figures, we found that the coupling efficiency of a structure consisting of a non-identical seven-core coupling is almost relatively high from a structure consisting of a three-core coupling, and therefore the latter is better than a structure consisting of two-core coupling. Where we find that there is a coupling between two cores without or with a slight penetration of neighbouring cores from among seven-core coupled, or perhaps we find that the coupling is completely absent between the seven cores in a multicore structure of seven cores and each core propagates independently and individually from its neighbours. While the structure consists of three-core coupled, we find a small coupling efficiency between two cores without or with remarkably simple penetration with other cores. Concerning the structure consisting of the coupled of two cores, we find that the coupling efficiency between them is completely non-existent, and each core propagates independently from the other. Depending on the results, we demonstrated that the coupling efficiency depends on the number of the coupled cores. It changes with the change of the number of cores that exist within a multicore structure, even if all the cores are different diameters.



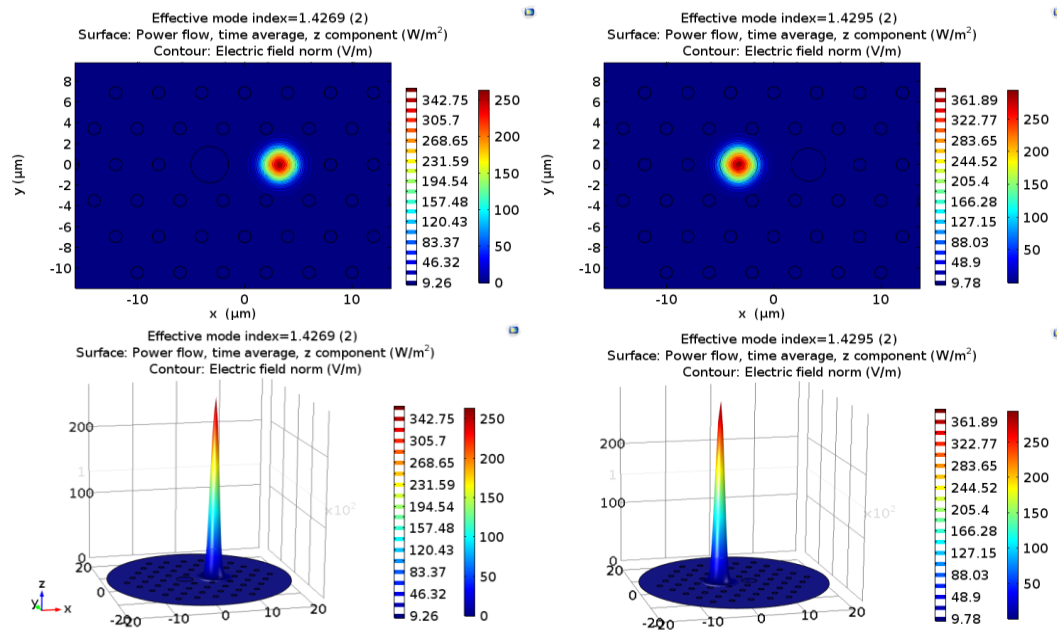
**Figure 1.** Cross-section of two-core PCF coupler with a three-ring hexagonal lattice, the geometry of PCF design characterized by the structure parameters, such as the core diameters of 3.2  $\mu\text{m}$ , 3.5  $\mu\text{m}$ ; hole pitch  $\Lambda=4$   $\mu\text{m}$ , hole diameter  $d=1.16$   $\mu\text{m}$ , the air-filling fraction  $d/\Lambda=0.29$  and core separation  $D=2.5$   $\mu\text{m}$ , at the wavelength  $\lambda=1.55\mu\text{m}$ , respectively. (a) Insert core material; (b) Insert cladding material; (c) Mesh triangular finite element.



**Figure 2.** Cross-section of three-core PCF coupler with a three-ring hexagonal lattice, the geometry of PCF design characterized by the structure parameters, such as the core diameters of  $3.2\ \mu\text{m}$ ,  $3.5\ \mu\text{m}$ ,  $3.8\ \mu\text{m}$ ; hole pitch  $\Lambda=4\ \mu\text{m}$ , hole diameter  $d=1.16\ \mu\text{m}$ , the air-filling fraction  $d/\Lambda=0.29$ , and core separation  $D=2.5\ \mu\text{m}$  at the wavelength  $\lambda=1.55\ \mu\text{m}$ , respectively. (a) Insert core material; (b) Insert cladding material; (c) Mesh triangular finite element.

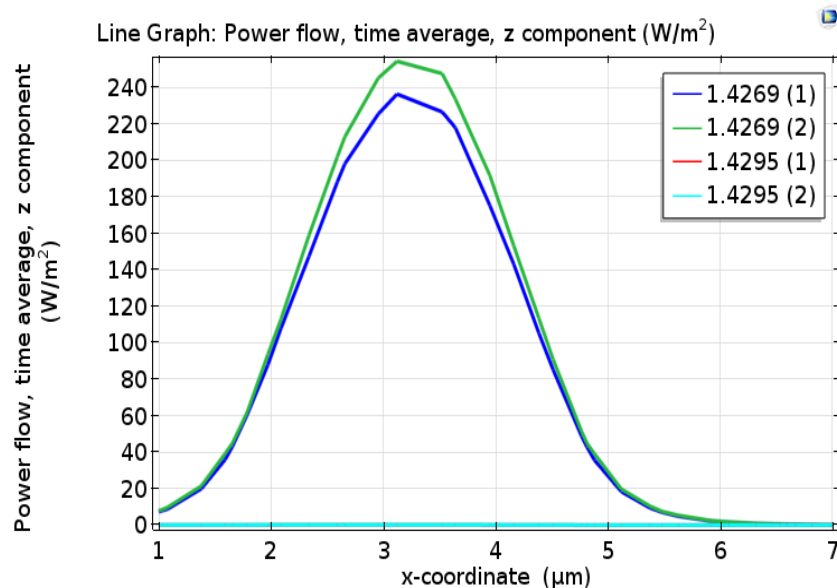


**Figure 3.** Cross-section of seven-core PCF coupler with a five-ring hexagonal lattice, the geometry of PCF design characterized by the structure parameters, such as the core diameters of  $3.2\ \mu\text{m}$ ,  $3.47\ \mu\text{m}$ ,  $3.48\ \mu\text{m}$ ,  $3.49\ \mu\text{m}$ ,  $3.5\ \mu\text{m}$ ,  $3.51\ \mu\text{m}$ ,  $3.52\ \mu\text{m}$ ; hole pitch  $\Lambda=5.6\ \mu\text{m}$ , hole diameter  $d=4.48\ \mu\text{m}$ , the air-filling fraction  $d/\Lambda=0.8$  and core separation  $D=2\ \mu\text{m}$  at the wavelength  $\lambda=1.55\ \mu\text{m}$ , respectively. (a) Insert core material; (b) Insert cladding material; (c) Mesh triangular finite element.



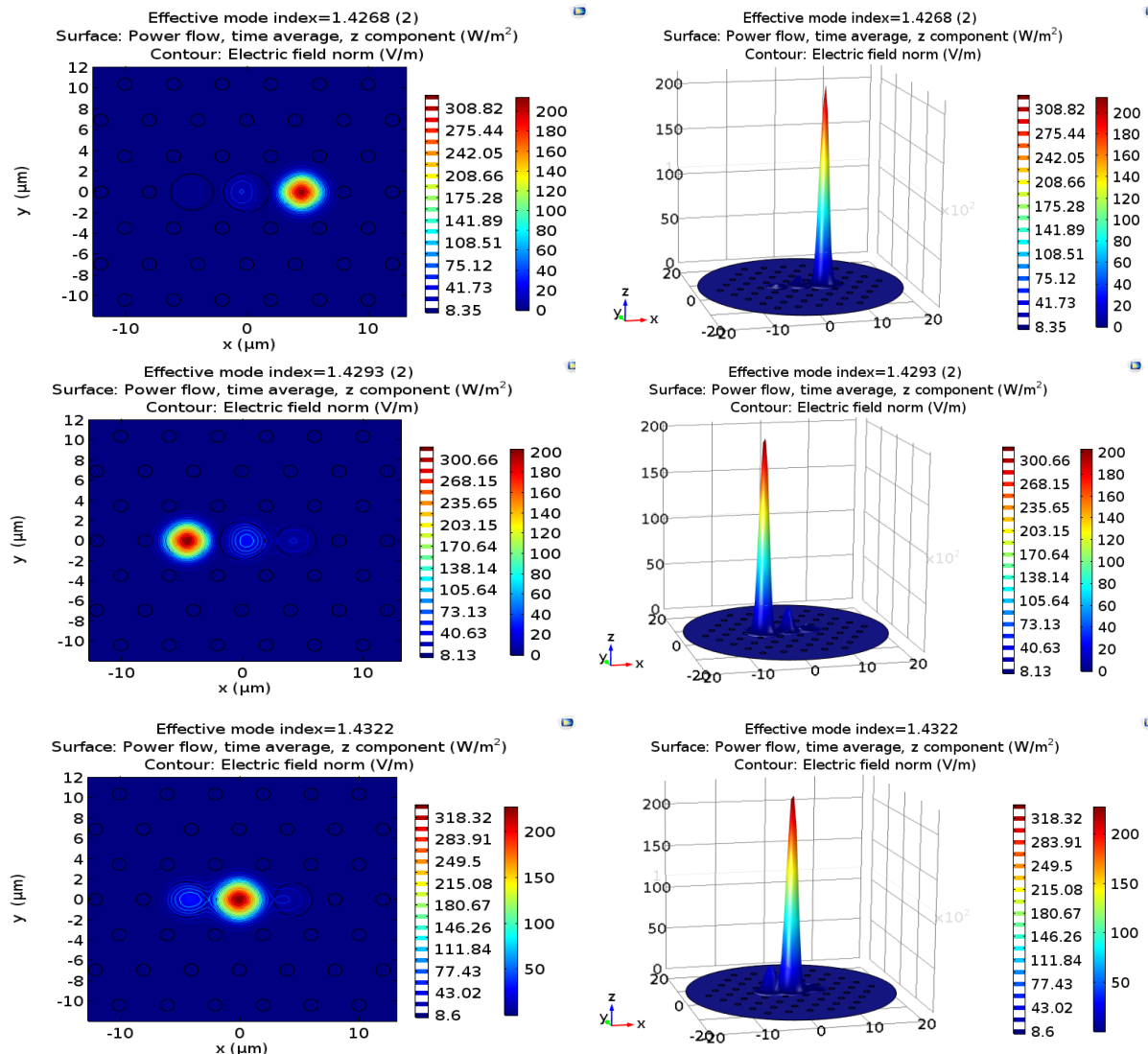
**Figure 4.** Power flow of the z-component ( $\text{W/m}^2$ ) in each core of a two-core of the PCF coupler overlapping with the contour of distributions of electric field norm  $|E|$  ( $\text{V/m}$ ). The effective mode indices corresponding to the modes of two-core are 1.4295 and 1.4269, respectively.

Figure 5 represents a structure consisting of two cores, and each core has two modes represented in the form of coloured lines. For example, the first core represents its modes in blue and green colour lines, while the second core represents in light blue and red colour lines, we notice that there is no coupling between the modes of these cores, and consequently the two cores to become decoupled and individual in isolation so that the propagation of light in each core is independent of the other inside the structure.



**Figure 5.** The evolution of the power flow of each core represents in the distribution of the unique power for two-core PCF where each core supports two propagation modes when input is to the central core.





**Figure 6.** Power flow of the z-component ( $\text{W/m}^2$ ) in each core of a three-core of the PCF coupler overlapping with the contour of distributions of electric field norm  $|E|$  ( $\text{V/m}$ ). The effective mode indices corresponding to the modes of three-core are 1.4268, 1.4293, and 1.4322.

Represent figure 7 a structure consisting of three cores, and each core has two modes, i.e., six modes of three cores, and these modes represent in colour lines. For example, first, we see the modes of the central core represent yellow and pink lines with a slight penetration of the modes of the left cores presented in green and blue lines and also with a very slight penetration of the mode of the right core that represented in light blue and red. Second, the modes of the left core have the same situation as the first case. While the modes of the right core are presented in colours with light blue and red, these modes are decoupled and independent from other modes of the cores and remain isolated inside the structure.

Figure 9 a structure consisting of seven cores and each core has two modes, i.e., fourteen modes of seven cores, and these modes are represented via the colour lines. We found that there is coupling only between the four modes of the two adjacent cores, which are represented in green and blue and also in light blue and pink. Alternatively, we found each core decoupled from others, and light propagation in each core is independent, representing this in the rest extended colours.



Figure 10 shows the refractive mode index that corresponds to the random changes in the diameters of the cores within multicore PCF, such as a multicore structure consisting of two-core coupled that possess random diameters such as  $3.2\ \mu\text{m}$  and  $3.5\ \mu\text{m}$ , and the refractive indices for corresponding modes of these cores are 1.4269 and 1.4295. While the structure consists of three-core coupled with random core, such as  $3.2\ \mu\text{m}$ ,  $3.5\ \mu\text{m}$ , and  $3.8\ \mu\text{m}$ , the refractive indices of the core modes are 1.4268, 1.4293, and 1.4322. For a structure that consists of seven-core coupled with the random core as  $3.2\ \mu\text{m}$ ,  $3.47\ \mu\text{m}$ ,  $3.48\ \mu\text{m}$ ,  $3.49\ \mu\text{m}$ ,  $3.5\ \mu\text{m}$ ,  $3.51\ \mu\text{m}$ , and  $3.52\ \mu\text{m}$ , the refractive index coefficients are 1.4418, 1.4427, 1.4427, 1.4427, 1.4428, 1.4428, and 1.4428, respectively.

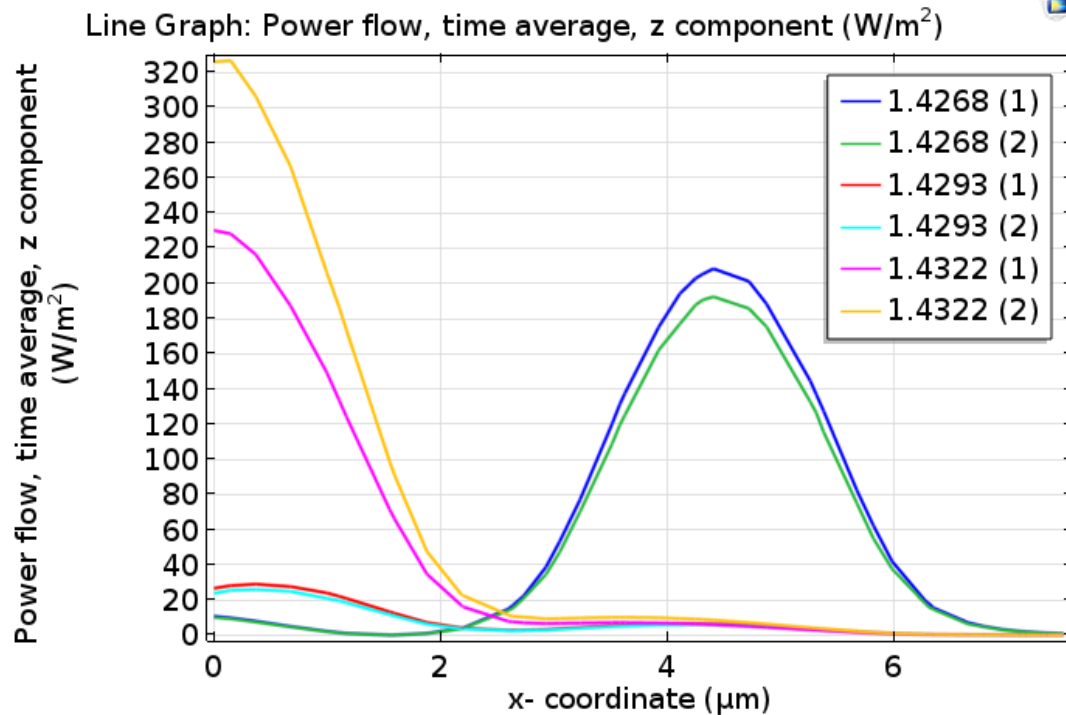


**Figure 7.** The evolution of the power flow of each core represents in the distribution of the unique power for three-core PCF, where each core supports two propagation modes when input is to the central core

## 5. Conclusion

COMSOL MULTIPHYSICS software is based on the finite element method we are using to simulate multicore photonic crystal fibres with different structures and introducing random variation into their core diameters. The results we showed that the coupling efficiency is changed in the multicore structures by happening anisotropy in their core diameters and depends this on the amount of the change in the core diameter and how can this change affects the coupling properties between the cores, and then on the coupling efficiency between them. Our results indicate that the coupling efficiency in the multicore structures is possible to improve by increasing the number of cores within it; otherwise, the light-independent core propagation with or without a little penetration of adjacent cores, where the power of each mode is almost totally focused on one core as individual cores, hence coupling efficiency between cores becomes approximately zero, as a result, all the coupling can be neglected and this is shown in our results when we have reduced the number of the cores to two cores. This characteristic could be excellent in an application such as multiplexing–demultiplexing.

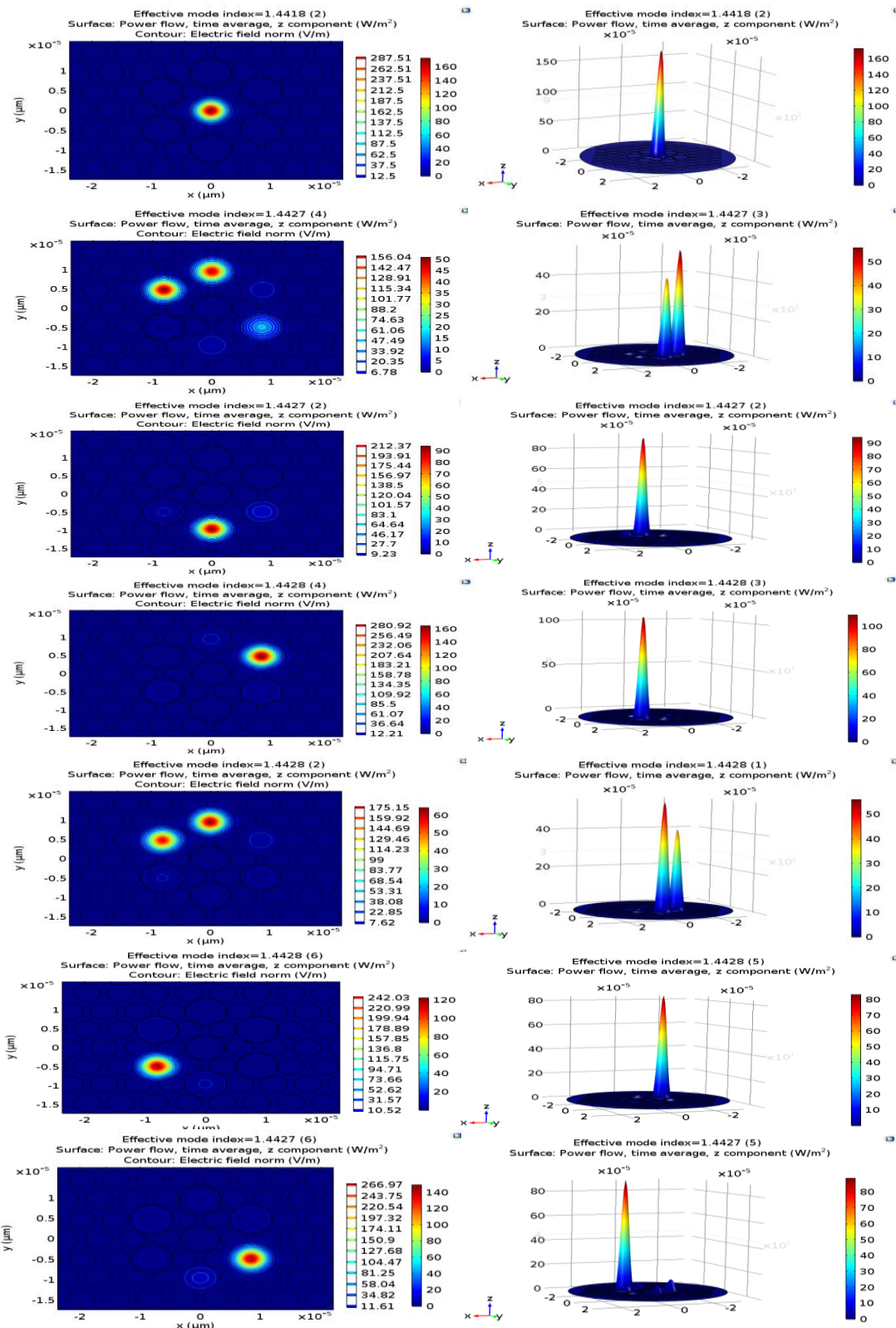


**Figure 8.** Power flow of the z-component (W/m<sup>2</sup>) in each core of a seven-core of the PCF coupler overlapping with the contour of distributions of electric field norm  $|E|$  (V/m). The effective mode indices corresponding to the modes of seven-core are 1.4418, 1.4427, 1.4427, 1.4427, 1.4428, 1.4428, 1.4428, respectively

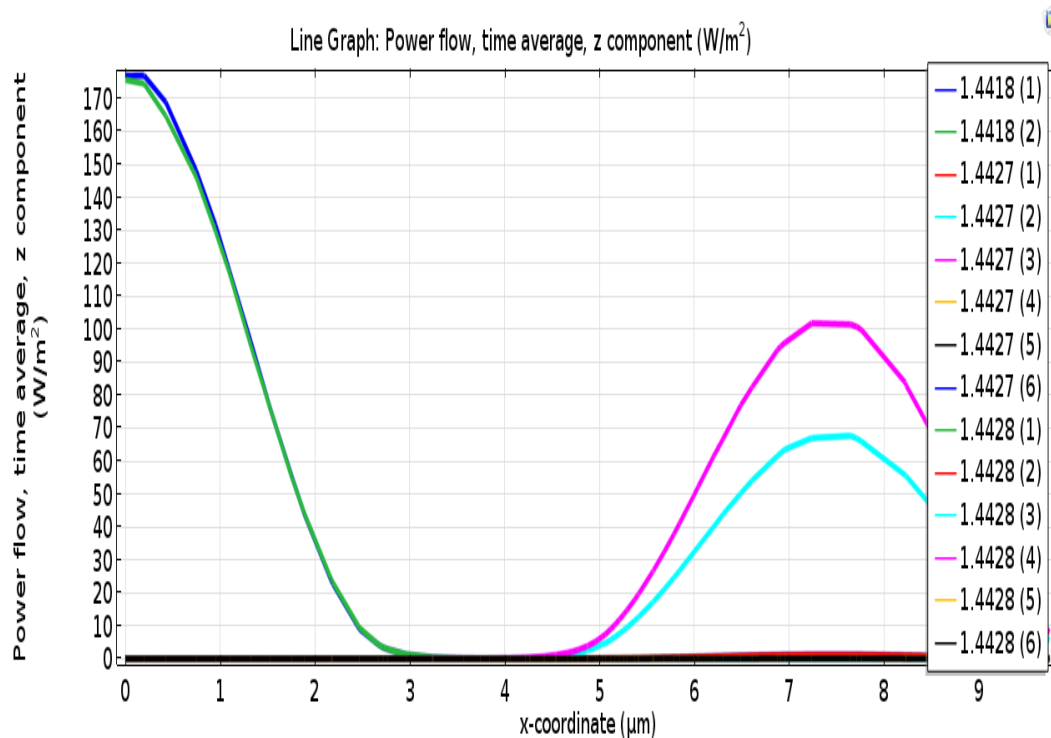


**Figure 9.** The evolution of the power flow of each core represents in the distribution of the unique power for two, three, seven-core PCF, where each core supports two propagation modes when input is to the central core.

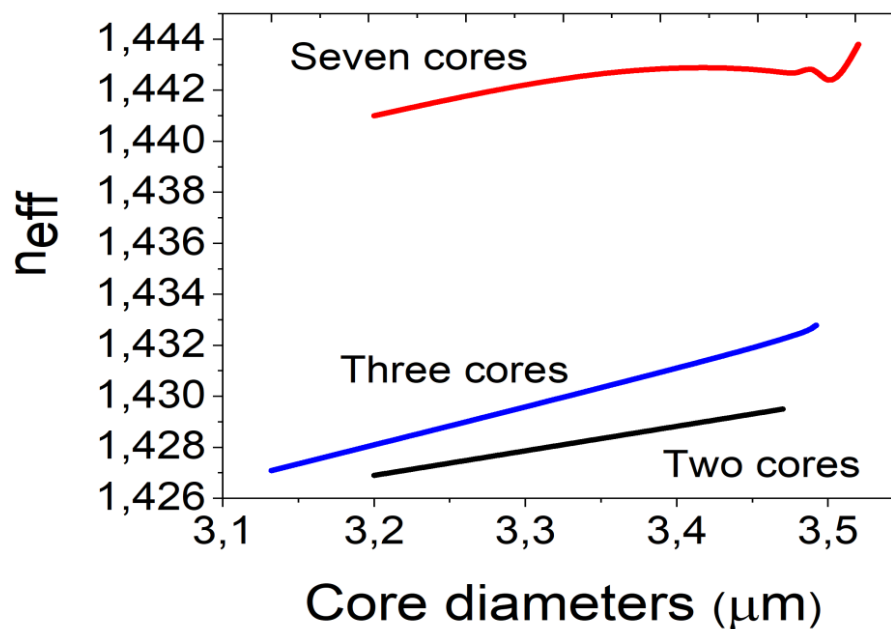


**Figure 10.** Scheme showing the relationship between the refractive mode index and the random changes of the diameters of the core in the multicore PCF for structures consisting of two, three, and seven cores.

## Acknowledgments

This work was partially supported by the Republic of Iraq Ministry of High Education & Scientific Research scholarship (MoHESR Grant No. 16408). And also, author acknowledges the University of Muenster-department of physics, Germany to support.

## References

- [1] Reichenbach K L and Xu C 2005 *J. Opt. Exp.* **25** 10336-10348
- [2] Saitoh K, Sato Y and Koshiba M 2003 *J. Opt. Exp.* **24** 3188-3195
- [3] Yu X, Liu M, Chung Y, Yan M, Shum P 2006 *J. Opt. Commun* **260** 164-169
- [4] He H and Wang L 2013 *J. Optik* **124**. 5941-5944
- [5] Khan K R and Wu T X 2008 *J. ACES* **3** 215
- [6] Mohammed M 2019 *Proc. Int. CMES Conf. on Computational Methods in Engineering Science (Poland)* **ISBN: 978-83-7947-386-1** 74-87 [www.biblioteka.pollub.pl/wydawnictwa](http://www.biblioteka.pollub.pl/wydawnictwa)
- [7] Rohini P K, Raja A S and Sunda D S 2015 *J. IJARTET* **ISSN2394-3777**, 186-190
- [8] Mothe N, Bin P D 2009 *J. Opt. Exp* **18** 15778-15788
- [9] Yuan C and Shi J 2010 *J. Opt. Commun* **283** 2686-2689
- [10] Reichenbach K L and Xu C 2007 *J. Opt. Exp.* **15** 2151-2156
- [11] Ahmad A K and Khalifa Z 2020 *Proc. Int. AIP Conf. on Physical Sciences* **2213** 020131 <https://doi.org/10.1063/5.0000121>
- [12] Andres J, Dario N, Gonzalez E P T and Reyes E 2020 *J. Photon.* **7** 3
- [13] Parto M, Amen M, M-ALI M, Amezcua R, LI G and Christodoulides D N 2016 *J. Opt. Lett* **41** 1917-1920
- [14] Szostkiewicz L, Napierala M, Ziolkowicz A, Pytel A and Tenderenda T 2016 *J. Opt. Lett.* **41** 3759-3762
- [15] Hanna I and Maciej A 2019 *J. Fibers* **7** 109
- [16] Younis B, Heikal A, Mohamed F and Obayya S 2018 *J. Opt. Soc. Am. B* **35** 1020-1029
- [17] Uthayakumar T, Raja R V J, Porsezian K and Grelu P 2015 *J. IEEE Photon.* **7** 1—11
- [18] Reyes-Vera E, Úsuga J, Gómez-Cardona N and Varón M 2016 *Proc. Int. Conf. on Latin America Optics and Photonics Conference (OSA)*
- [19] Mohammed M, Ahmad K A 2020 *J. Rafidain Sci. Online* **ISSN 2664-2786** <https://rsci.mosuljournals.com>.
- [20] Mohammed M, Ahmad K A 2020 Analysis of light propagation in identical and non-identical multicore photonic crystal fibers *J. AL-Nahrain of Sci.* **Ref.:11088**
- [21] Wenhua R and Zhongwei T 2016 *J. Optik* **127** 3248-3252
- [22] Xia C, Eftekhar M A, Correa R A, Lopez J A, Schulzgen A, Christodoulides D and Li G 2016 *J. Quantu. Electron.* **22** 4401212